RSC Advances

REVIEW

View Article Online
View Journal | View Issue

Check for updates

Cite this: *RSC Adv.*, 2018, **8**, 12573

Fluorescent probes for the detection of magnesium ions (Mg^{2+}): from design to application

Min Liu,[ab] Xia Yu,[b] Ming Li,[c] Naixuan Liao,[b] Anyao Bi,[b] Yueping Jiang,[a] Shao Liu,[a] Zhicheng Gong*[a] and Wenbin Zeng *[b]

Received 30th January 2018
Accepted 21st March 2018

DOI: 10.1039/c8ra00946e

rsc.li/rsc-advances

Magnesium ions (Mg^{2+}) play essential roles in various physiological and pathological processes, its abnormal homeostasis in cells is related to many diseases, such as diabetes, neuromuscular disorders, hypertension and other cardiovascular disorders. Investigation on the regulation of magnesium in cellular processes has attracted considerable interest in the past several decades. Among those reported strategies, fluorescent imaging technology has become a powerful and cost-effective tool for the real-time monitoring of magnesium distribution, uptake and trafficking, due to its superior features of high sensitivity and non-invasiveness, as well as excellent spatial and temporal fidelity. Herein, we critically summarize the progresses in the intracellular magnesium detection with fluorescent imaging probes. Our discussion focuses on the recent contributions concerning fluorescent imaging probes for mapping magnesium in biological processes. All the candidates are organized according to their acceptor structures. The sensing mechanisms of fluorescent probes are also highly taken into account. Challenges, trends and prospects of fluorescent imaging technology in magnesium detection are also set forth.

Open Access Article. Published on 03 April 2018. Downloaded on 1/9/2025 5:36:55 PM.
This article is licensed under a Creative Commons Attribution-NonCommercial 3.0 Unported Licence.

1. Introduction

The magnesium ion (Mg^{2+}) is one of the most abundant essential elements in cells and plays a critical role in numerous cellular processes such as cell proliferation, cell death, enzyme-driven biochemical reactions, channel regulation, stabilization of DNA conformation and signal transduction.[1–3] There are approximately 300 enzymatic reactions mediated by Mg^{2+} in cells, and the concentration change of intracellular Mg^{2+} is believed to regulate the metabolism of cells.[4] In the majority of mammalian cells, intracellular free Mg^{2+} usually ranges from 0.5 mM to 0.7 mM, maintained by Mg^{2+} transport across the cell membrane, intracellular buffering and compartmentation into organelles.[5] In medical settings, hypomagnesemia can result from various causes including hypertension, diabetes, osteoporosis, metabolic syndrome, neuronal injury, cell senescence and antitumor efficacy of chemotherapeutics. By contrast, hypermagnesemia occurs less frequently than other common diseases, however, it associates significantly with chronic renal failure and even results in cardiac arrest in extreme cases.[6,7] In addition, magnesium sulfate is presently employed to treat numerous conditions such as arrhythmias, myocardial infarction and eclampsia.[8] Therefore, it is of great value and urgency to develop simple, rapid and efficient analytical methods to detect magnesium mobilization, distribution and concentration changes in cells.

Over the last few decades, several conventional analytical methods have been put forward to measure Mg^{2+} in either fixed or live samples. These methods have respective benefits and drawbacks and can be exploited with variable levels of confidence in studies of specific issues. Atomic absorption spectroscopy (AAS) developed by Australian chemist Walsh in the 1950s (ref. 9) has been historically the first and most frequently used technique to detect magnesium in acidic extracts of biological samples. The introduction of AAS partially obviated methodological limitations: the system made it possible to measure the level of magnesium in all biological samples, with a lower detection limit of 10 mM. However, AAS could only better our understanding of magnesium metabolism to some extent. In fact, investigating the physiological dynamics of Mg^{2+} at the cellular level needs techniques that ascend detection of Mg^{2+} movements across the diversiform compartments of a living cell. Radioactive isotopes (^{27}Mg and ^{28}Mg) were originally used to measure magnesium fluxes but have been abandoned on account of biohazard, short half-life and very high production costs. They are currently replaced by their stable counterparts (^{25}Mg or ^{26}Mg), which can be used in assessment of exchangeable magnesium pool masses as well as the evaluation of magnesium status and fluxes in animals and humans.[10] However, the method is costly and demands of detection by mass spectrometry (or better, ICP-MS), which is not easily accessible.

[a]*Department of Pharmacy, Institute of Hospital Pharmacy, Xiangya Hospital, Central South University, Changsha 410008, P. R. China . E-mail: gongzhicheng@csu.edu.cn*
[b]*Xiangya School of Pharmaceutical Sciences, Central South University, Changsha, 410013, P. R. China. Fax: +86-731-82650459; Tel: +86-731-82650459. E-mail: wbzeng@hotmail.com*
[c]*Changsha Stomatological Hospital, Changsha 410000, P. R. China*

Open Access Article. Published on 03 April 2018. Downloaded on 1/9/2025 5:36:55 PM.
This article is licensed under a Creative Commons Attribution-NonCommercial 3.0 Unported Licence.

Another sophisticated technique is phosphorus nuclear magnetic resonance spectroscopy (^{31}P-NMR), which depends on the fact that most magnesium in the cytosolic matrix is bound to ATP (adenosine triphosphate). When magnesium is bounded to ATP, it shifts the resonance frequencies of signals (chemical shift) coming from the three phosphoric groups of the molecule. Due to the chemical equilibrium between bound and free magnesium, the chemical shift of ATP signals is a function of free Mg^{2+} concentration. ^{31}P-NMR offers the unique opportunity to measure *in vivo* cytosolic Mg^{2+} concentration in several tissues and has provided new hints on magnesium homeostasis and its involvement in the cellular bioenergetics of human brain and skeletal muscle.[11] However, this method requires cumbersome sample pretreatment, time-consuming and complicated instruments. What's more, no information on intracellular magnesium distribution can be derived.

Due to the weaknesses of these methods, it inspires the creation of new analytical methods to help further our understanding of the distribution, uptake, and trafficking of Mg^{2+} in living systems.[12] Hence, fluorescent imaging technologies were developed and stand out as the most effective approach because of its simplicity, high sensitivity, excellent spatial–temporal resolution, fast response and non-invasiveness. Over the last decades, a boom of fluorescence imaging techniques have been witnessed among the most powerful platforms for dynamic behaviour determination and real-time observation in a single living cell,[13] which were also expected to be used in magnesium research. As a result, a variety of novel fluorescent probes for detection of Mg^{2+} have been reported. Together with the rapid development of confocal laser scanning and two-photon microscopy (TPM) techniques, fluorescence methods now provide a robust tool to visualize and measure Mg^{2+} in three dimensions, even deep into tissues.

To date, a plethora of fluorescent probes for Mg^{2+} have been developed and this research field has become very active and exuberant. Therefore, a systematic survey of progress in the rapid development of fluorescent probes for Mg^{2+} is highly demanded. Herein, we will focus on the recent progress in the creation of novel fluorescent imaging probes for Mg^{2+} and their applications in cell biology. Firstly, to gain a better understanding of the rational design approaches and discuss how the fluorescence probes react with the analytes, we will present and outline the general principles of designing effective fluorescent imaging probes for biological applications. Then, we will discuss advances in Mg^{2+} fluorescent imaging probes, which are classified according to different types of Mg^{2+}-selective binding sites, for highly specific sensing and detecting Mg^{2+} in cellular systems. In the end, we will conclude with a discussion of the reality and future challenges in this field from the perspective of available probes for fluorescence imaging detection of cellular Mg^{2+}.

Min Liu received his MS degree in 2014. Now he is a research assistant at Department of Pharmacy, Xiangya Hospital, Central South University (CSU). His current research interests are mainly in developing fluorescent chemosensors, molecular recognition and its application.

Xia Yu received her PhD in College of Pharmacy, Marburg University (2013). She joined CSU as an associate professor in 2016. Her current research interests focus on novel natural product discovery/structural modification, biosynthesis and application.

Ming Li received her PhD in Xiangya School of Medicine, Central South University. She acts as an associate professor in Changsha Stomatological Hospital. She is interested in pursuing modern technologies in clinical application.

Naixuan Liao is an undergraduate student in Xiangya School of Pharmaceutical Science, Central South University (CSU). She is currently engaging in scientific research under the supervision of Prof. Wenbin Zeng.

Anyao Bi was graduated from Xiangya School of Pharmaceutical Science, Center South University (CSU) in 2017. He is currently pursuing his PhD under the guidance of Prof. Wenbin Zeng. His research interests focus on the development of small fluorescent probes for living and environment system imaging.

Yueping Jiang obtained his PhD in Chinese Academy of Medical Sciences and Peking Union Medical College (2015). Currently he is a research assistant at the department of pharmacy of Xiangya Hospital, CSU. His current research interests are mainly in developing natural product fluorescent probes and biochemical application.

Shao Liu is a professor and deputy director of the Department of Pharmacy, Xiangya Hospital, CSU. His current research interests focus on drug development, drug testing new technology developments and the application of drug imaging probes.

Zhicheng Gong is a professor and director of the Department of Pharmacy, Xiangya Hospital, CSU. His current research interests focus on the drug epidemiology, clinical pharmacy and molecular oncologic pathology.

Wenbin Zeng obtained his PhD in Chemistry at the University of Muenster, Germany (2004). He joined CSU as a full professor in 2009. His current research interests focus on the development of novel fluorescent probes and sensors, and multimodal molecular imaging platforms for molecular imaging, theranostics and biomedical application.

 This journal is © The Royal Society of Chemistry 2018

Open Access Article. Published on 03 April 2018. Downloaded on 1/9/2025 5:36:55 PM.
This article is licensed under a Creative Commons Attribution-NonCommercial 3.0 Unported Licence.

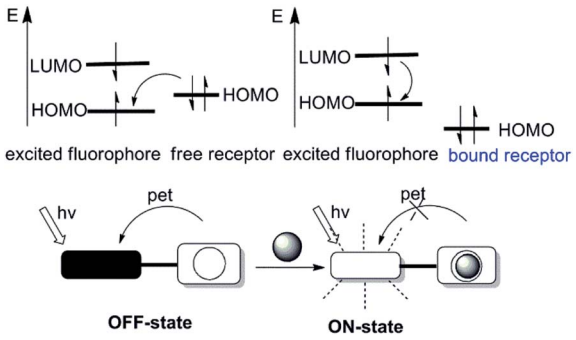

Fig. 1 Schematic illustration of the mechanism based on reductive-PET.

2. The general design principles of functional fluorescent probes

Many photophysical processes (quenching *via* collision, photoinduced electron transfer, exciplex formation, photoinduced proton transfer, energy transfer and *etc*) may be responsible for the fluorescence changes (excitation and emission spectra, quantum yield, fluorescent lifetime and *etc*) upon binding of the analyte by the probes.[14,15] The most widely utilized fluorescence signaling mechanisms in the design of probes will be briefly discussed in this section.

2.1 Photoinduced electron transfer (PET)

Photoinduced electron transfer (PET) is possible the cause of fluorescence quenching, when the PET process is followed by a nonluminescent process back to the normal state.[16,17] The PET process can be illuminated picturesquely based on the molecular orbital theory, therefore becomes a powerful tool to expound the fluorescence "on–off" switching of fluorescent probes. Fluorescent probes on the basis of PET are often structured as fluorophore-spacer-chelator constructs. In this pattern, an aliphatic spacer separates the fluorophore and chelator, thus electronically disconnect the π-electron systems of them. According to the electron accepting or donating relationships between fluorophore and chelator in one fluorescent probe, PET can be subdivided into the reductive PET and the oxidative PET.[18] This review will focus on the reductive PET due to its frequent use in the design of fluorescent probes (as depicted in Fig. 1). In reductive PET, the fluorophore is reduced while the chelator is oxidized, that is the chelator acts as the electron donor (*e.g.*, the amine group) and the fluorophore serves as the electron acceptor. During the reductive PET process, photo-excitation promotes an electron from the HOMO (the highest occupied molecular orbital) of the fluorophore to its LUMO (the lowest unoccupied molecular orbital). Subsequently, the reaction between the fluorophore and the analytes induces either the appearance or removal of the "nearby" orbital between HOMO and LUMO of the fluorophore, leading to fluorescence quenching or enhancement, respectively.

2.2 Intramolecular charge transfer (ICT)

The intramolecular charge transfer (ICT) strategy for cation sensing was introduced by Valeur.[19] Probes based on ICT are featured by conjugation of an electron-donating unit to an electron-accepting unit in one molecule to rise a "push–pull" π-electron system in the excited state,[20] which have been extensively used for cation sensing. While the electron-donating part interacts with an analyte, the electron-donating character of the probe decreases, generating a blue shift in the absorption spectrum. In contrast, an evident red shift is observed when the ICT becomes more developed owing to the interaction of an analyte with the electron-accepting part (as described in Fig. 2). Besides, changes in the fluorescence lifetimes and quantum yields are also observed. Up to now, a great number of fluorescent imaging molecules are derived from this ICT mechanism by changing either the electron-donating, electron-withdrawing ability or π-conjugation degree of the fluorophores to interact with the target analyte.

2.3 Excited-state intramolecular proton transfer (ESIPT)

Excited-state intramolecular proton transfer (ESIPT) has also been adopted for designing fluorescent imaging probes because

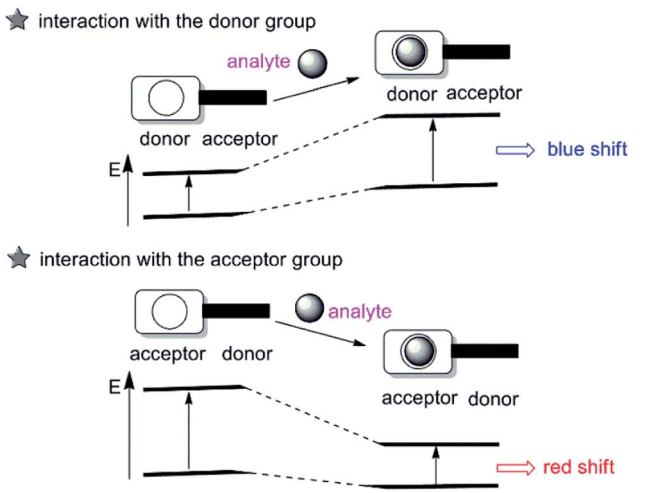

Fig. 2 Schematic representation of the intramolecular charge transfer (ICT) process.

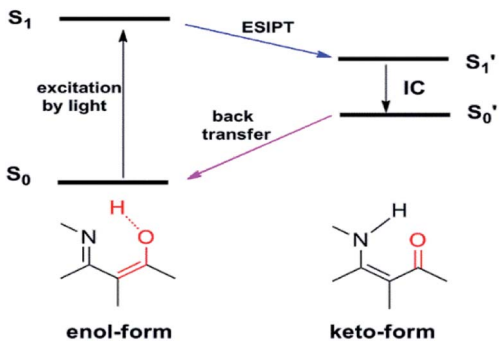

Fig. 3 Schematic representation of the excited-state intramolecular proton transfer (ESIPT) process.

Open Access Article. Published on 03 April 2018. Downloaded on 1/9/2025 5:36:55 PM.
This article is licensed under a Creative Commons Attribution-NonCommercial 3.0 Unported Licence.

of its unique and excellent spectral sensitivity to the environmental medium. ESIPT process typically involves a fast proton transfer from a proton donor (often hydroxyl or amino unit) to an acceptor group (usually either carbonyl oxygen or imine nitrogen) atom in the excited state of a fluorophore mediated by an intramolecular hydrogen bond.[21] A pictorial representation of ESIPT process is depicted in Fig. 3.

Owing to the transformation between the enol and keto form in the ESIPT-based system, as such, the ESIPT process not only radically reduces the photochemical reactivity of the excited molecules, but also significantly enhances their photostability. On top of this, a large manifest Stokes shift can also be observed. Therefore, the ESIPT process is quite suitable for designing fluorescent imaging probes requiring spectral shift for selective detection.

2.4 Fluorescent resonance energy transfer (FRET)

Fluorescence resonance energy transfer (FRET) mechanism comprises energy transfer between a pair of fluorophores that serve respectively as energy donor and acceptor.[22,23] FRET is a distance-dependent interaction between the electronic excited states of two chromophores in which excitation energy is non-radiatively transferred from a donor chromophore to an acceptor chromophore *via* nonradiative dipole–dipole coupling (as represented in Fig. 4). In those transfer processes, several vibronic transitions in the donor have approximately equivalent energy to those in the acceptor. Molecules in which FRET is operative are quintessentially used to artificially increase the Stokes shift. As applied in sensing applications, the emission of the donor at relatively short wavelengths serves to activate emission of the acceptor at longer wavelengths with the ratio of the fluorescence intensities of the donor and acceptor emissions modulated by the target analytes. To obtain a high FRET efficiency, it is required that spectral overlap between the donor emission and the acceptor absorption spectrum is substantial.[24] Many FRET-based fluorescent probes have been created subsequent to these pioneering efforts for the ratiometric detection of metal ions, such as Hg^{2+},[25] Zn^{2+}.[26] So far, no FRET-based fluorescent probes for Mg^{2+} have been reported, which suggests that it is a hard nut to crack in this field.

3. Fluorescent probes for magnesium ions based on different binding sites

Besides the fluorescence signaling mechanisms, there are several important characteristics of fluorescent imaging probes must to be tuned when selecting or designing aprobe for imaging the analyte in living cellular systems, such as the excitation/emission wavelength, photostability, fluorescence quantum yield, fluorescence lifetime and so on. Conceivably, the most significant factor to consider when choosing a fluorescent probe is its binding affinity, which mainly depends on the acceptor. The acceptor, in other words, is the selective binding sites and dictates the sensitivity to molecular/ion recognition. To be applied in living cellular systems, a high-affinity Mg^{2+} binding probe should be selective for Mg^{2+} over

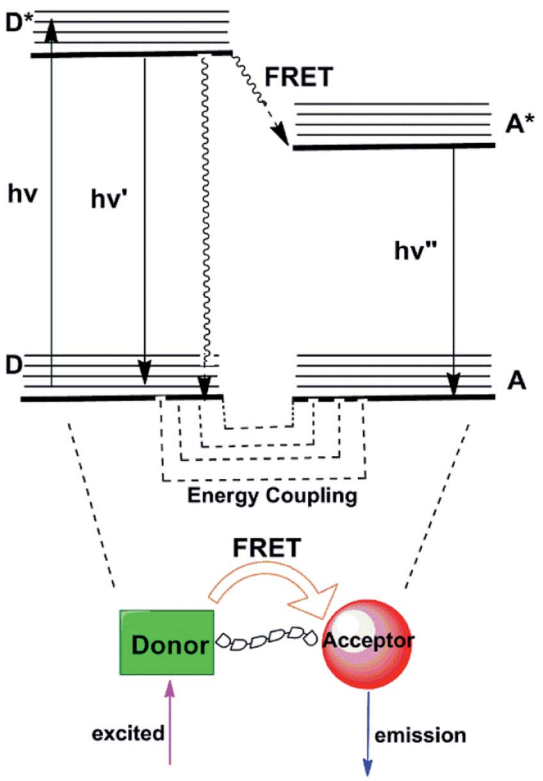

Fig. 4 Schematic representation of the energy transfer process based on FRET.

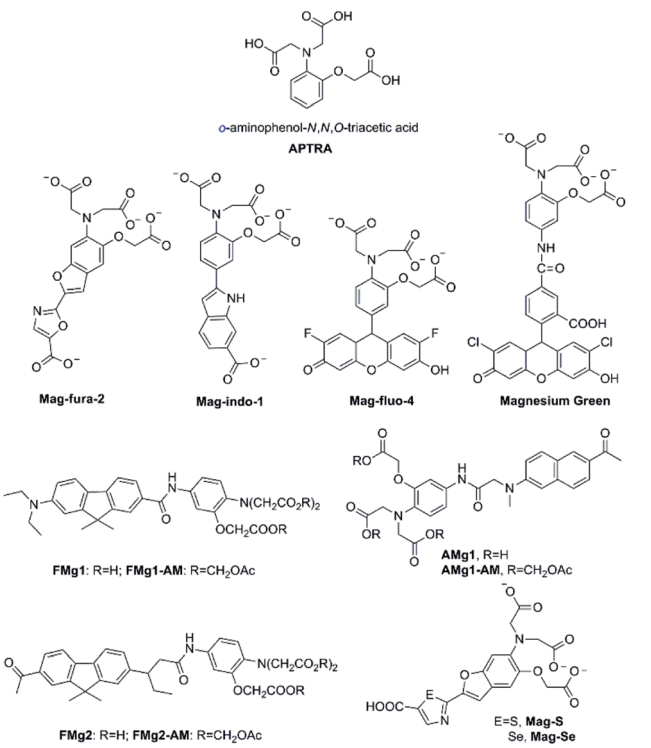

Fig. 5 Chemical structure of APTRA and fluorescent probes for Mg^{2+} featuring APTRA as the Mg^{2+}-selective binding site.

This journal is © The Royal Society of Chemistry 2018

Open Access Article. Published on 03 April 2018. Downloaded on 1/9/2025 5:36:55 PM. This article is licensed under a Creative Commons Attribution-NonCommercial 3.0 Unported Licence.

other biologically abundant ions, which exist at much higher cellular concentrations. In the further section, we will try to provide a critical overview of Mg^{2+} fluorescent probes based on different binding sites known by now, with particular regard to the latest advances.

3.1 Fluorescent probes for Mg^{2+} based on *o*-aminophenol-*N*,*N*,*O*-triacetic acid (APTRA)

The *o*-aminophenol-*N*,*N*,*O*-triacetic acid (APTRA) structure, which is the most common acceptor, is generally deemed to be the Mg^{2+}-selective binding site (its structure is shown in Fig. 5). The first widely available fluorescent Mg^{2+} probe was anchored in the chemical design by Roger Tsien, who rationally devised fluorescent Ca^{2+} probes for intracellular use in the late 1970s.[27,28] The prototype of such Ca^{2+} probes was modified as fluorescent probes for measuring cytosolic free Mg^{2+} by Robert London.[29,30] One modification method is that fluorinated derivatives of the chelator APTRA have been designed and synthesized for use as ^{19}F-NMR indicators of free cytosolic Mg^{2+} concentration. Another way is that the APTRA structure is modified around the furan ring, resulting in the fluorescent probe **Mag-fura-2** (as shown in Fig. 5).[31] From then on, many other dyes purported to be selective for Mg^{2+} have been put forward, and most of them are simply analogues of the corresponding Ca^{2+} probes: for example, **Mag-indo-1** (analogue of indo-1) and **Magnesium Green** (analogue of calcium green) (see Fig. 5 for their chemical structures). It's obvious that the chemical structure of those probes contain a common APTRA unit as Mg^{2+}-selective binding site.

Mag-fura-2, the first fluorescent Mg^{2+} probe, was designed to visualize and understand intracellular Mg^{2+} distributions.[31] **Mag-fura-2** is excited by ultraviolet (UV) light (λ_{max} = 369 nm) showing a blue shift to 330 nm in absorption spectra upon Mg^{2+} binding, and also a shift in emission spectrum in the visible region from 511 nm in Mg^{2+}-free medium to 491 nm at saturating Mg^{2+} concentrations. The binding dissociation constant for Mg^{2+} is 1.9 mM. **Mag-Fura-2** has been exploited to measure the intracellular Mg^{2+} concentration in cells from the muscle, heart, liver, and nervous system.[32–35]

Thereafter, **Mag-indo-1** has been synthesized on the strength of identical molecular design as **Mag-fura-2**.[36] **Mag-indo-1** has a dissociation constant (K_d) of 2.7 mM for Mg^{2+} and is excited by UV light to emit fluorescence in the visible region. **Mag-fura-2** undergoes a palpable shift in excitation wavelength after binding to Mg^{2+}, whereas **Mag-indo-1** presents a shift in both its excitation and emission wavelengths. The K_d of **Mag-indo-1** for Mg^{2+} is lower than that of **Mag-fura-2** (the parameter is shown in Table 1), which is conducive for the measurement of high spikes in intracellular Mg^{2+}, for example the temporal analysis of Ca^{2+}-induced Mg^{2+} mobilization in neurons or the glutamate-stimulated Mg^{2+} concentration change.[37–39]

Later, several other fluorescent probes which possess the APTRA group as the binding site for Mg^{2+} have been developed, such as **Mag-fluo-4** and **Magnesium Green**.[40,41] The remarkable feature of those probes compared to the aforementioned ones is that they are excited by visible light (see Table 1) rather than UV irradiation which is regarded to be more cytotoxic.[42] The maximum excitation and emission of **Magnesium Green** are 490 nm and 520 nm, respectively. Upon binding to Mg^{2+}, the fluorescence intensity of **Magnesium Green** increases without any shift in the wavelength. Moreover, **Magnesium Green** presents a higher affinity for Mg^{2+} compared to both **Mag-fura-2** and **Mag-indo-1**. In biological applications, **Magnesium Green** has been exploited to probe intracellular Mg^{2+} for the exploration of the binding of free Mg^{2+} by the bacterial SecA protein and the investigation of ATP hydrolysis in spontaneously contracting cardiomyocytes.[43,44]

Unfortunately, Mg^{2+} fluorescent probes possessing APTRA as binding site lack the appropriate selectivity for Mg^{2+} over Ca^{2+}, which implies that Ca^{2+} become a confounding factor in Mg^{2+} detection when Ca^{2+} concentrations exceed about 1 μM.[45] Therefore, Ca^{2+} disturbs the accuracy of Mg^{2+} measurement and limits the interpretation of the read-out eventually. To deal with this problem, Bong Rae Cho and co-workers developed efficient two-photon fluorescent probes **FMg1** and **FMg2** (structures are shown in Fig. 5) to simultaneously monitor Mg^{2+}/Ca^{2+} activities.[46] Through using BCaM and **FMg2**, one can simultaneously detect Ca^{2+}/Mg^{2+} activities in live cells and even in live tissues at a depth of more than 100 μM for long periods of time without photobleaching artifacts. What is worth mentioning is that BCaM, a two-photon probe for near membrane Ca^{2+} was also designed by the same research team.[47] In **FMg1** and **FMg2**, the

Table 1 Basic characteristics of the fluorescent Mg^{2+} probes based on APTRA binding site

Probes	Fluorophore	$\lambda_{max,abs}$ (nm)	$\lambda_{max,em}$ (nm)	K_d (Mg^{2+})[a]	K_d (Ca^{2+})	Ref.
Mag-fura-2	Benzofuran	369/330	511/491	1.9 mM	25 μM	31
Mag-indo-1	Indole	349/330	480/417	2.7 mM	35 μM	36
Mag-fluo-4	Fluorescein	490/493	None[b]/517	4.7 mM	22 μM	40
Magnesium-Green	Fluorescein	506/none	None/531	2.0 mM	6.0 μM	41
FMg1	Fluorene	362/none	540/none	1.5 mM	8.8 μM	46
FMg2	Fluorene	368/none	555/none	1.7 mM	9.8 μM	46
AMg1	Naphthalene	365/none	485/none	1.4 mM	9.0 μM	48
Mag-S	Furan	396/330	572/547	3.2 mM	48 μM	49
Mag-Se	Furan	412/360	584/562	3.3 mM	41 μM	49

[a] K_d, dissociation constant; if not otherwise stated, K_d values were measured in aqueous buffers; for details please see the cited references. [b] None represents the spectral no change.

Open Access Article. Published on 03 April 2018. Downloaded on 1/9/2025 5:36:55 PM.
This article is licensed under a Creative Commons Attribution-NonCommercial 3.0 Unported Licence.

APTRA group serves as the receptor for Mg^{2+}, while 2-acetyl-7-diethylamino-9, 9-dimethyl-9*H*-fluorene and 2-diethylamino-7-nonanoyl-9,9-dimethyl-9*H*-fluorene acts as the fluorophore, respectively. The acetoxymethyl (AM) ester form of them (**FMg1-AM** and **FMg2-AM**) can passively diffuse through the plasma membrane and readily stand enzymatic hydrolysis to reform the metal-ion probe inside the cell. **FMg1** and **FMg2** display absorption maxima at 362 nm and 368 nm with fluorescence maxima at 540 nm and 555 nm, respectively. When Mg^{2+} is added to **FMg1** and **FMg2** in MOPS buffer, the fluorescence intensity increases remarkablely without impact on absorption spectra, which may be a result of the blocking of the PET from APTRA to fluorophore upon chelation with Mg^{2+}. The K_d values of **FMg1** and **FMg2** for Mg^{2+} are 1.5 mM and 1.7 mM, respectively (see Table 1). **FMg2-AM** in combination with BCaM are utilized as two-photon probes to investigate Mg^{2+}/Ca^{2+} activities in HepG2 cells by dual-color imaging.

As noted above, the two-photon microscopy (TPM) is able to visualize the distribution of intracellular metal ions in living cells and tissues. TPM utilizes two photons with lower energy as the excitation source, is getting increasingly prevalent among biologists owing to several distinct advantages. Two-photon probes offer numerous unique benefits over one-photon probes, from increased penetration depth (>500 mm), lower tissue autofluorescence and self-absorption to reduced photodamage and photobleaching. In fact, the first two-photon fluorescent probe **AMg1** for Mg^{2+} was also initially developed by Bong Rae Cho research team in 2007.[48] **AMg1** (as showed in Fig. 5) chooses 2-acetyl-6-(dimethylamino)naphthalene as the two-photon chromophore and APTRA to be the Mg^{2+}-selective binding site. The maximum excitation wavelength of **AMg1** is 365 nm and its maximum emission wavelength is 498 nm. Once binding to Mg^{2+}, **AMg1** undergoes a slight change in the absorption spectrum. In contrast, when Mg^{2+} concentrations increase, a dramatic enhancement in the fluorescence is observed probably due to the blocking of the PET process by metal-ion complexation. The fluorescence enhancement factor is measured to be 17 in the presence of 100 mM Mg^{2+}. In addition, the K_d for Mg^{2+} is determined to be (1.4 ± 0.1) mM, which is close to the intracellular concentration of free Mg^{2+}. Therefore, **AMg1** can detect intracellular free Mg^{2+} of live cells and tissue. The carboxylic acid moieties of **AMg1** were converted into AM esters (**AMg1-AM**) to enhance the cell permeability. The authors assert that **AMg1-AM** characteristic should allow eliminating a source of error in Mg^{2+} quantification by discriminating the contribution of membrane-bound uncleaved ester-probe.

The desire for more superior photophysical properties of Mg^{2+} fluorescence probes, especially in terms of longer excitation and emission wavelengths, led to the development of the red-shifted fluorescent probes for Mg^{2+} by incorporating sulfur or selenium in the azole moiety of 'fura' fluorophores, as named **Mag-S** and **Mag-Se** (structures are shown in Fig. 5).[49] The molecular design of **Mag-S** and **Mag-Se** is based on the strategy that the incorporation of heavier chalcogens into the structure of the **Mag-fura-2** probe would help shift their excitation and emission to longer wavelengths, becoming more submissive for live cell fluorescence imaging of Mg^{2+}. **Mag-S** and **Mag-Se** show a promising result in reality. **Mag-S** and **Mag-Se** display excitation maximum at 392 nm and 410 nm in the free-state, respectively, while the two probes show emission maximum at 572 nm and 584 nm in unbound form, respectively. Hence, a single replacement of O by S or Se in the structure of the fluorophore generates a bathochromic shift greater than 60 nm in the emission of the probe. Both **Mag-S** and **Mag-Se**'s responses to Mg^{2+} show a significant hypochromatic shift in the fluorescence excitation and emission spectra. The separation between excitation bands for the metal-free and bound probe anchored to the electron poorer thiazole and selenazole is dramatically larger than that of the oxazole derivative. This feature is desirable for ratiometric imaging and the test for responding of **Mag-S** for the ratiometric measurement of Mg^{2+} in HeLa cells was performed. Recently, the same research group using **Mag-S** as the parent probe introduced a clever two-step strategy for *in situ* anchoring and activation of fluorescent sensing Mg^{2+} within intracellular organelles of choice.[50] Step one, they choose append a tetrazine moiety to **Mag-S** through a fluorogenic reaction; step two, as trained bicyclononyne in the structure of fluorophore covalently linked to a genetically encoded HaloTag fusion protein of known cellular localization. Experiments proved that the sensing system could realize the aim for the ratiometric detection of Mg^{2+} in target organelles in HEK293T cells. The labelling strategy is, furthermore, fully compatible with live cell imaging and enables the real time visualization of changes in metal ion distribution involved in cellular processes, providing a valuable tool for tracking changes in magnesium distribution that to date have been an unsolved mystery in the cell biology of Mg^{2+}.

However, the other photophysical properties of the probes do not improve significantly. For example, the interference of Ca^{2+} or other biologically relevant metal ions is not negligible. Moreover, the fluorescence quantum yield is lower. On top of these, the dissociation constants of **Mag-S** and **Mag-Se** decrease slightly in comparison to **Mag-fura-2**. To sum up, the chalcogen replacement strategy may open the doors to enhance red-shifted ratiometric detection for other biologically relevant ions.

3.2 Fluorescent probes for Mg^{2+} based on charged β-diketone binding site

There is a great demand for the development of optimized Mg^{2+} fluorescent probes to achieve the dynamic and three-dimensional imaging of intracellular Mg^{2+}. Alternative acceptor featuring a charged β-diketone or related β-dicarbonylbidentate binding motifs has been efficiently incorporated into fluorescent probes for the measurement of Mg^{2+} (as shown in Fig. 6).

As early as 2002, Suzuki *et al.* reported the development of two novel Mg^{2+} fluorescent imaging probes **KMG-20-AM** and **KMG-27-AM** (as shown in Fig. 6), in which AM is an acetoxymethyl group, grounded on a coumarin possessing a charged β-diketone substructure.[51] Both probes have a β-hydroxycarboxylic acid group and an aromatic amino group combined

 This journal is © The Royal Society of Chemistry 2018

Open Access Article. Published on 03 April 2018. Downloaded on 1/9/2025 5:36:55 PM.
This article is licensed under a Creative Commons Attribution-NonCommercial 3.0 Unported Licence.

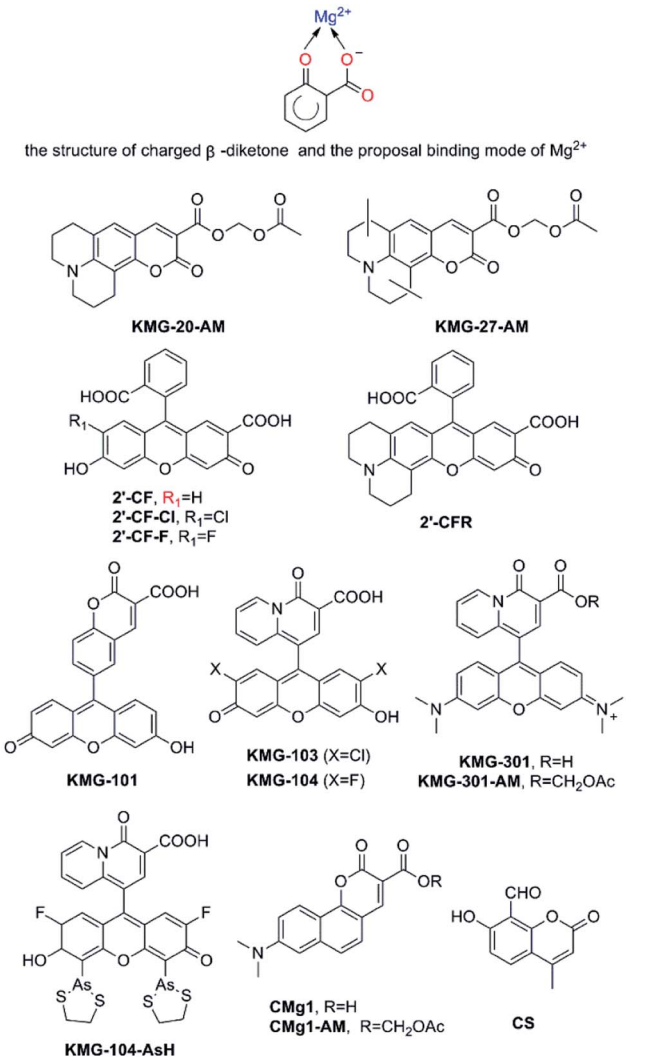

Fig. 6 Proposal binding mode of Mg^{2+} based on a charged β-diketone and fluorescent probes for Mg^{2+} featuring a charged β-diketone as Mg^{2+}-selective binding site.

by a conjugated π-electron system, which not only frees bright fluorescence detection from the influence of protons under neutral conditions, but also brings about a large fluorescence spectral change subsequent to formation of the Mg^{2+} complexes inasmuch as the ICT process. These fluorescent probes give rise to a red shift from 425 nm to 445 nm in the absorption spectra due to formation of a complex with Mg^{2+}. Besides, the fluorescence spectrum also presents a red shift from 485 nm to 495 nm and a rise in fluorescence intensity after Mg^{2+} complex formation. Moreover, the probes display a "seesaw-type" fluorescent spectral change with the isosbestic point at 480 nm as a result of the light excitation at 445 nm, implying that ratiometry can be used for the measurement. The K_d of **KMG-20-AM** is 10.0 mM. This value for Mg^{2+} is three times higher than for Ca^{2+}, and the selectivity of Mg^{2+} over Ca^{2+} is more than 200 times higher than that of other Mg^{2+} fluorescent molecular probes such as **Mag-fura-2** and **Magnesium Green**. In addition, **KMG-20-AM** and **KMG-27-AM** are proved to be successfully applied in the measurement of intracellular Mg^{2+} concentration imaging with fluorescent microscopy in living cells. Take PC12 cells as an example, the addition of **KMG-20-AM** and **KMG-27-AM** into PC12 cells led to a strong fluorescence in the cytoplasm and a weak fluorescence in the nuclear region. After treatment with high-K^+ medium, the fluorescence intensity increases owing to increasing intracellular Mg^{2+} concentrations. High K^+ can depolarize the cell membrane and activates several ion channels, therefore, $Mg^{2+}$is released from intracellular stores, making it possible for**KMG-20-AM** and **KMG-27-AM** to image Mg^{2+} distribution successfully. As another application of **KMG-20-AM**, Park and co-workers developed Mg^{2+}-sensitive nanoparticles for intracellular use by PEBBLE (probe encapsulated by biologically localized embedding) technology.[52] The particles are stable but show affinities and spectroscopic limitations analogous with those of **KMG-20AM**.

Fluorescein and rhodamine are known to be excitable at long wavelength, and have a high fluorescence quantum yield in an aqueous medium, as is generally used in biological experiments.[53] Nagano and co-workers developed four novel fluorescent Mg^{2+} probes, **2′-CF**, **2′-CF-Cl**, **2′-CF-F** and **2′-CFR** (these probe are shown in Fig. 6). All of them contain 2′-carboxyfluorescein or its derivatives as fluorophore, and a carboxyl group at the 2′-position to make up a β-keto acid moiety as the Mg^{2+} chelating site.[54] Those probes could be used in the confocal microscope, however, they showed a lower affinity for Mg^{2+} (K_d = 15.8 mM of **2′-CF**, other parameters are shown in Table 2) and suffered from strong pH interference, therefore, the project were forced to be abandoned. Then, the focus shifts to the KMG series. Similar to **KMG-20-AM**, these compounds possess a charged β-diketone as a specific binding site for Mg^{2+}, which is attached to the 9′-position of xanthene (as presented in Fig. 6), resulting in the novel Mg^{2+} fluorescent probes, **KMG-101**, **-103**, **-104**, and **KMG-301**.[55,56] This molecular design results in an intensive off-on-type fluorescent response toward Mg^{2+}, showing both the highly sensitive photoinduced electron transfer-type (PET) response and Mg^{2+} affinity modification, as well as the allowance of Ar^+ laser excitation. Among the four probes mentioned above, **KMG-104** possesses the most desirable properties, for it can be excited by the 488 nm line of Ar lasers and its fluorescence emission rises along with Mg^{2+} concentrations, while the absorption spectrum only displays minor changes. In addition, its K_d is about 2.1 mM. Therefore, comparable to that of APTRA-based probes, the new dye has a better affinity for Mg^{2+} and is suitable to detect free intracellular Mg^{2+}. No response of it to alkali metals is observed yet. More interestingly, **KMG-104** displays a K_d for Ca^{2+} of 7.5 mM, which is much higher than the resting physiological free Ca^{2+} concentration. Therefore, the selectivity of this probe for Mg^{2+} over Ca^{2+} is much superior to that exhibited by **Mag-fura-2** and **Mag-fluo-4**. Moreover, the fluorescence of **KMG-104** appears to be insusceptible by pH changes in the range from 6.0 to 7.6. In order to simplify cell loading, **KMG-104-AM**, a membrane-permeable probe of AM ester form of **KMG-104** has also been synthesized. The probe was successfully incorporated into PC12 cells through microinjection method. By using a confocal microscope, the intracellular three-dimensional Mg^{2+}

Open Access Article. Published on 03 April 2018. Downloaded on 1/9/2025 5:36:55 PM. This article is licensed under a Creative Commons Attribution-NonCommercial 3.0 Unported Licence.

Table 2 Basic characteristics of the fluorescent Mg^{2+} probes based on a charged β-diketone binding site

Probes	Fluorophore	$\lambda_{max,abs}$ (nm)	$\lambda_{max,em}$ (nm)	K_d (Mg^{2+})[a]	K_d (Ca^{2+})	Ref.
KMG-20	Coumarin	425/445	485/495	10.0 mM	33.3 mM	51
KMG-27	Coumarin	425/445	483/494	9.80 mM	30.0 mM	51
2′-CF	Fluorescein	477/493	508/515	15.8 mM	ND[b]	54
2′-CF-Cl	Fluorescein	481/500	518/523	9.1 mM	ND	54
2′-CF-F	Fluorescein	471/493	518/522	12.8 mM	ND	54
2′-CFR	Rhodamine	535/544	564/567	29.5 mM	ND	54
KMG-101	Fluorescein	492/493	519/516	100 mM	150 mM	55
KMG-103	Fluorescein	515/517	533/533	1.8 mM	6.3 mM	55
KMG-104	Fluorescein	502/504	523/523	2.1 mM	7.5 mM	55
KMG-301	Rhodamine	560/563	570/600	4.5 mM	ND	56
KMG-104-AsH	Fluorescein	520/521	540/540	1.7 mM	100 mM	58
CMg1	Naphthalene	413/443	556/559	1.3 mM	3.6 mM	59
CS	Coumarin	343/350	473/485	1.75 mM	ND	60

[a] K_d, dissociation constant; if not otherwise stated, K_d values were measured in aqueous buffers; for details please see the cited references. [b] ND, not determined.

distributions were successfully imaged with the **KMG-104-AM** probe. **KMG-104** was adopted to detect Mg^{2+} transients upon mitochondrial depolarisation, and this led to the hypothesis that mitochondria could be intracellular magnesium stores.[57] Features of **KMG-104** in terms of excitation spectrum, fluorescence enhancement and ion selectivity make this probe become one of the most promising alternatives to detect free Mg^{2+} by live cell imaging.

In order to combine the fluorescent probe **KMG-104** with a protein and explore the mobilization as well as underlying mechanisms of Mg^{2+}, **KMG-104-AsH** has been designed and developed (as shown in Fig. 6). **KMG-104-AsH** consists of the highly selective fluorescent Mg^{2+} probe and a tetracysteine peptide tag (TCtag), which can be genetically incorporated into any protein.[58] After the combination, **KMG-104-AsH** has a highly selective affinity for Mg^{2+} (K_d for Mg^{2+} = 1.7 mM, K_d for Ca^{2+} = 100 mM), with its fluorescence intensity increases by more than 10-fold. Furthermore, fluorescent imaging of intracellular Mg^{2+} in HeLa cells reveals that this FlAsH-type Mg^{2+} sensing probe is membrane-permeable and bound specifically to tagged proteins, such as TCtag-actin and mKeima-TCtag targeted to the cytoplasm and the mitochondrial intermembrane space. This probe is a promising tool for elucidating the dynamics and mechanisms of intracellular localization of Mg^{2+}.

Developing an efficient two-photon probe for the detection of Mg^{2+} ions in living cells and live tissues is a very useful strategy. Bong Rae Cho and his research group designed another two-photon probe **CMg1**. In contrast to the APTRA binding site in **AMg1**, **CMg1** contains a strong donor–acceptor pair in the cyclic planar framework to facilitate the intramolecular charge transfer (ICT) for high two-photon cross-section and an integral β-keto acid as the Mg^{2+}-binding site to increase water solubility, while maintaining a small molecular weight for optimal cell permeability.[59] **CMg1** can be excited at 880 nm and its spectral properties was dramatically influenced by the lipophilicity of the solvent, deciphered as a better metal ion binding in a more hydrophobic environment. Indeed, the binding affinity of **CMg1** for Mg^{2+} increases gradually with sodium dodecyl sulfate (SDS) concentration up to the critical micellar concentration, and then remains constant at 1.3 mM. Interestingly, the titration curves displayed the complexation between **CMg1** and Mg^{2+} in a 10 mM SDS solution and were found to be similar to that in ionophore-treated cells. Thus SDS micelles seem to represent a suitable model for the intracellular environment. While the K_d of **CMg1** for Mg^{2+} is comparable to that of probes whose binding site is APTARA such as **Mag-fura-2** and **Mag-fluo-4**, its K_d for Ca^{2+} is only 3.6 mM, showing obvious selectivity for Mg^{2+} over Ca^{2+}. However, the selectivity is still not as good as that of **KMG-104**. Fortunately, thanks to the order of magnitude of typical free Mg^{2+} and Ca^{2+} intracellular concentrations, **CMg1** can effectively measure free intracellular Mg^{2+} with no interference from Ca^{2+}. Apart from this, no response toward either alkali metal ions (Na^+, K^+) or transition-metal ions (Zn^{2+}, Fe^{2+}, Mn^{2+}, Cu^{2+}, Co^{2+}) has been discovered. In addition, **CMg1** is capable of selectively detecting intracellular Mg^{2+} in living Hep3B cells and imaging endogenous stores of free Mg^{2+} at 100–300 μM depth in live tissues using two-photon microscopy.

Coumarin and its derivatives have been extensively used as organic dyes to design fluorescent probes. **CS** was a good example, Gupta *et al.* using coumarin derivatives, 4-methyl-7-hydroxy-8-formyl coumarin, a simple molecule served as a selective probe for Mg^{2+}.[60] (as presented in Fig. 6) **CS** shows a remarkable enhancement and a small red shift of 12 nm from 473 to 485 nm in fluorescence emission upon complexation with Mg^{2+}. The phenolic OH and the oxygen atom of carbonyl group have been proved to be the binding sites of **CS** to Mg^{2+} to form a rigid β-dicarbonyl bidentate binding syetem. The limit of detection of Mg^{2+} is found to be much lower as 0.43 μM and **CS** may be a practical probe for detection of Mg^{2+} in analytical as well as environmental and biological samples.

3.3 Fluorescent probes for Mg^{2+} based on crown ether binding site

Crown ether has been a popular receptor for alkaline or alkaline earth metal ions owing to various sizes of cavities available as

 This journal is © The Royal Society of Chemistry 2018

Open Access Article. Published on 03 April 2018. Downloaded on 1/9/2025 5:36:55 PM.
This article is licensed under a Creative Commons Attribution-NonCommercial 3.0 Unported Licence.

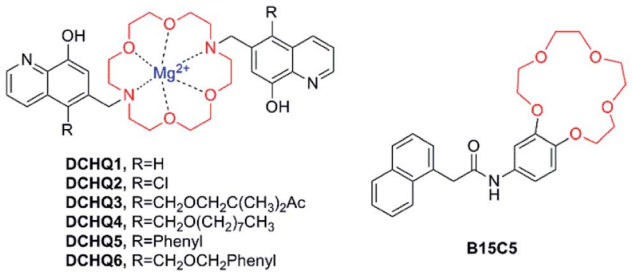

Fig. 7 Chemical structure of fluorescent probes for Mg^{2+} featuring crown ethers as the Mg^{2+}-selective binding site.

well as the effective chelation ability of the oxygen lone pairs for these "hard'' metal ions. The common types of crown ether include 15-crown-5 ether, 18-crown-6 ether and the diaza-18-crown-6 ether, in which two nitrogen atoms are inserted into the structure of 18-crown-6 ether. All of them possess the outstanding properties of metal ion coordination.

In 2007, Hama *et al.* published a report on the probe **B15C5** (as shown in Fig. 7),[61] which possesses benzo-15-crown-5 as recognition moiety and 1-naphthaleneacetamide as chromophore moiety. Its fluorescence emission showed a significant enhancement after the addition of Mg^{2+}, and a detectable, yet not as prominent, increase in the existence of other alkaline earth metal ions (Ca^{2+}, Sr^{2+}, Ba^{2+}). Nevertheless, at present this compound does not show a promising future, for the observation of its excitation and emission spectra in the UV range and spectroscopic characterisation in organic solvents, which are incompatible with biological samples.

8-Hydroxyquinoline (8-HQ) is deemed as the second Mg^{2+} chelation agent in significance after ethylene diaminetetraacetic acid (EDTA).[62] The most noteworthy characteristic of 8-HQ is its extremely low quantum yield in aqueous or organic solutions and the fluorescence enhancement arising from cation binding, which results in an intense yellow-green fluorescence. Furthermore, the fluorescence of the complex species varies with the environment and becomes brighter as lipophilicity increases.[63,64]

A significant and promising work had been accomplished by an Italian research group, who designed and developed a new family of fluorescent molecules for Mg^{2+} obtained by conjugation of a diaza-18-crown-6 ether with 8-hydroxyquinolines bearing various substituents (**DCHQ1-6**, Fig. 7).[65–69]

Among the panel of the novel synthesized DCHQ probes, various of groups are inserted into the 5-position of the **8-HQ** side arms to obtain diverse target probes. **DCHQ1** and **DCHQ2** were obtained by substitution of hydrogen atom and chlorine atom, respectively, while **DCHQ3** bears two terminal acetoxymethyl ester groups instead with the goal of enhancing cellular uptake and/or trapping efficiently. Furthermore, by bearing long alkyl chains on the 8-hydroxyquinoline side arms, **DCHQ4** obtains higher lipophilicity and, consequently, better affinity for membranes. Finally, one aromatic group each is inserted on the 8-HQ side arms to give **DCHQ5** and **DCHQ6**, conducing to the overall charge delocalization, in an attempt to bathochromic-shift the absorption and emission spectra with respect to the parent probe **DCHQ1**.

The photophysical properties of these probes have been extensively studied. Several probes exhibit a remarkable increase in fluorescence intensity in the existence of Mg^{2+} while other alkaline-earth ions induce no noticeable fluorescence increase. Probes in this family display an intense band at around 240–250 nm and a smaller and broader band at around 310–330 nm in free-state. The former can be ascribed to a π–π^* transition, while the latter shows a main charge transfer feature with charge density shifting from the hydroxyl oxygen atom to the quinolone.[66] All the compounds present a weak emission band at around 465–510 nm with low values of fluorescence quantum yields in free form, due to the presence of the nitrogen atom in the macrocycle and the 8-HQ derivative, which can be elucidated by the photoinduced electron transfer (PET) mechanisms. The increasement of Mg^{2+} can be observed in the absorption spectra of all the DCHQ derivatives, featuring the decrease of the bands centered at 240–250 and 310–330 nm as well as the appearance of new bands around 260–265 and 370–390 nm. These new bands are characterized by 8-HQ derivatives when the complexation process is accompanied by the deprotonation of the hydroxyl group in the 8 position.[70] Apart from this, Mg^{2+} binding causes a tremendous enhancement of the emission spectra for all the studied species, up to 20 times higher than the fluorescence intensity of the free ligand, which can be explained by the fact that PET is inhibited by complexation.

In order to investigate their affinity and photochemical behaviors in the presence of Mg^{2+} and other possible competitive ions, a systematic study of the probes have been performed. Interestingly, all the DCHQ derivatives presented identical trends with regard to complexation ability: no changes were observed either in absorption or emission spectra after the addition of Na^+, K^+, Ca^{2+}, Fe^{2+} and Fe^{3+}, indicating that these species do not form any complex with the DCHQ ligands. On the contrary, Hg^{2+}, Cu^{2+} and Ni^{2+} were efficiently bound to the molecules but constituted nonluminescent complexes. Among all the tested metal ions, only Mg^{2+}, Zn^{2+} and Cd^{2+} induced a prominent enhancement of the fluorescence in the system (See Table 3). However, Zn^{2+} and Cd^{2+} ions are not anticipated to give rise to substantial interference in total intracellular Mg^{2+} determination for the following reasons: (1) the intracellular concentration of Zn^{2+} is approximately 100 times lower than that of Mg^{2+}, not to mention that most of Zn^{2+} is bound to zinc fingers with relatively high association constants;[71] (2) Cd^{2+} is not present in non-poisoned cells.

Loading cell, and the distribution of the probes between cells and medium as well as the detection of Mg^{2+} by live cell imaging were further investigated. In analogy to **KMG-104**, the experiments were conducted by Kubota *et al.*[57] While **KMG-104** showed cytosolic free Mg^{2+} transients upon mitochondrial depolarization, an astonishingly similar enhancement in fluorescence in **DCHQ1**-loaded cells was found, despite differences of the binding affinities between them.[66] In addition, Chiara Marraccini *et al.* performed experiments with the DCHQ compounds by two-photon imaging in the study of intracellular

Open Access Article. Published on 03 April 2018. Downloaded on 1/9/2025 5:36:55 PM.
This article is licensed under a Creative Commons Attribution-NonCommercial 3.0 Unported Licence.

Table 3 Basic photophysical properities of the fluorescent Mg^{2+} probes based on crown ether binding site

Probes	Chromophore	$\lambda_{max,abs}$ (nm)	$\lambda_{max,em}$ (nm)	log K_a			Ref.
				Mg^{2+}	Zn^{2+}	Cd^{2+}	
DCHQ1	Hydroxyl-quinoline	244/244	505/505	5.02 ± 0.08^a	5.85 ± 0.06^a	9.39 ± 0.05^b	66
DCHQ2		245/245	510/510	ND[c]	ND[c]	ND[c]	66
DCHQ3		246/246	510/513	10.1 ± 0.1^b	6.12 ± 0.07^a	9.53 ± 0.05^b	68
DCHQ4		247/247	463/513	11.2 ± 0.4^b	6.50 ± 0.2^a	9.30 ± 0.06^b	68
DCHQ5		249/249	512/517	5.08 ± 0.06^a	6.60 ± 0.2^a	9.4 ± 0.2^b	69
DCHQ6		245/245	504/514	4.8 ± 0.4^a	5.80 ± 0.09^a	8.91 ± 0.06^b	68
B15C5	Naphthaleneacetamide	258/250	338/338	K_d (Mg^{2+}) = 2.9 μM, K_d (Ca^{2+}) = 1.3 μM			61

[a] Value obtained for 1 : 1 metal-to-ligand stoichiometry. [b] Value obtained for a 1 : 2 metal-to-ligand stoichiometry. [c] ND, the data of log K_a is not determined by reference; K_d values of **DCHQ1** and **DCHQ2** for Mg^{2+} are 44 μM and 73 μM, respectively.[64] If not otherwise stated, K_d values were measured in aqueous buffers; for details please see the cited references.

total Mg^{2+} distribution.[68] According to the results, the aromatic probe **DCHQ5** presented unique characteristics and appears to be a valuable and efficient candidate tool for the evaluation of total intracellular Mg^{2+} and understanding the homeostasis of this important element better. As an example of the sensitivity of **DCHQ5**, the participation of Mg^{2+} in multidrug resistance in human colon adenocarcinoma LoVo cells sensitive (LoVo-S) and resistant (LoVo-R) to doxorubicin was studied. The results revealed a higher Mg^{2+} concentration in LoVo-R cells.[69] Theseintriguing results indicate that the photochemical characteristics of **DCHQ** probes might be applied to detect Mg^{2+} movements across intracellular compartments, which is worth further investigation. What's amazing, in 2017 Lvova *et al.* developed novel all-solid-state optodes *via* inclusion inside PVC-based polymeric films of different DCHQ based receptors to perform fast monitoring of Mg^{2+}.[72]

3.4 Fluorescent probes for Mg^{2+} based on a Schiff base ligand

A Schiff base is a compound with the general structure $R_2C = NR'$. It derives from condensation of an aliphatic or aromatic amine and a carbonyl compound. In the realm of coordination chemistry, the Schiff base plays an important role and is commonly used as ligands to form coordination complexes with metal ions.[73] Recently, moderating the corresponding groups of C=N structure to construct fluorescent probes for Mg^{2+} were based on the combination action of fluorescence signaling mechanisms. For example, probe **SBL-1** (as shown in Fig. 8, take the first letter of each word in phrase: Schiff base ligand, named SBL) selectively recognizes Mg^{2+} due to rapid isomerization around the C=N bond,[74] meanwhile, the introduction of a hydroxyl to the adjacent nitrogen can induce excited state intramolecular proton transfer (ESIPT) to generate a keto tautomer with proficient Mg^{2+} binding capability, such as probe **SLB-2**, **-3**, **-4**, and **SLB-5**. They are also identified as the photo-induced electron transfer (PET) action from the lone pair of the sp^2 nitrogen to the fluorophore when the fluorescence could be quenched in coordination without Mg^{2+}, however, when probes bind to Mg^{2+}, these processes will be blocked.

SBL-1, a novel probe, which was designed and developed by Ray and co-workers,[74] connected two different coumarin derivatives through an imine linkage to form a metal binding site in the middle of fluorescence signaling system. The molecule possesses satisfying photophysical properties, including a large Stokes shift, visible excitation and emission wavelengths as well as little or no interference from other metal ions. Disappointingly, this indicator is completely useless for

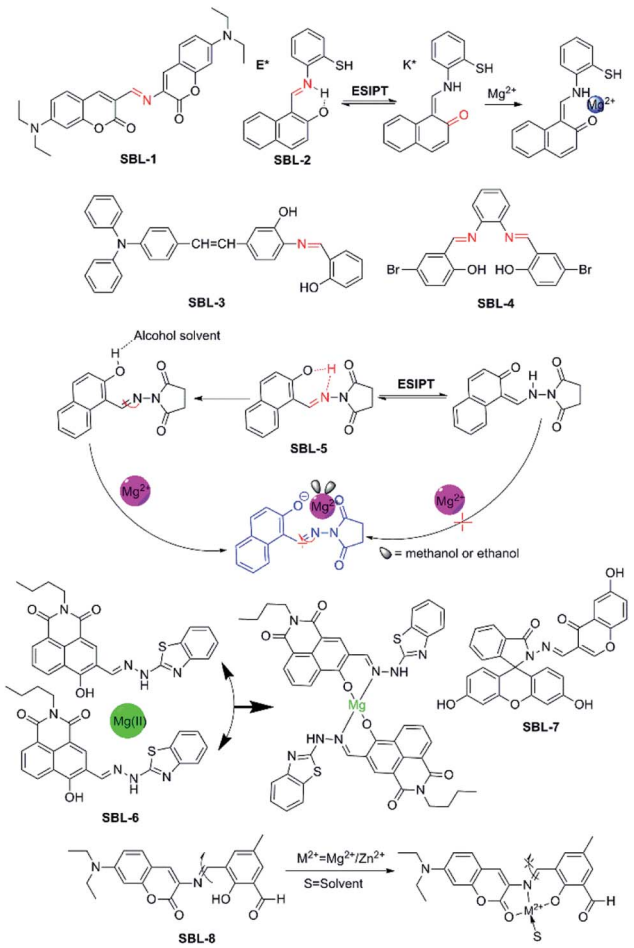

Fig. 8 Chemical structures of fluorescent probes for Mg^{2+} feature a Schiff base ligand as the receptor group and the proposal complexation mechanism of fluorescent probes with Mg^{2+}.

This journal is © The Royal Society of Chemistry 2018

Open Access Article. Published on 03 April 2018. Downloaded on 1/9/2025 5:36:55 PM. This article is licensed under a Creative Commons Attribution-NonCommercial 3.0 Unported Licence.

biological applications, because its emission dramatically decreases upon the addition of water, and entirely vanishes in 10% v/v water, which makes this indicator completely futile for biological applications.

SBL-2, which was designed and developed by Narinder Singh and colleagues,[75] has been constructed for the ratiometric recognition of Mg^{2+} in semi-aqueous solution at pH 7.0. This probe with a Schiff base ligand in structure undergoes ESIPT process which can provide dual channel emission to realize ratiometric determination of Mg^{2+}, along with the keto tautomer as an efficient receptor for Mg^{2+}. The fluorophore exists preferentially in the enol form and is stabilized in the ground state by an intramolecular six-membered ring H-bonding motif. Upon excitation at 275 nm, the excited enol form (E*) is transformed into the excited keto tautomer (K*) arised from ESIPT. This process results in an emission band (band at 355 nm) with a large Stokes shift. The keto form (K) returns to the enol form *via* a reverse proton transfer after decaying to the ground state (the proposed responding model with Mg^{2+} is showed in Fig. 8). Perturbations to the intramolecular arrangement by means of intermolecular H-bonding interactions or variations in solvent polarity have been extensively studied. **SBL-2** displays good selectivity of Mg^{2+} over other metal ions and does not suffer from interference by Ca^{2+} in particular and can measure Mg^{2+} ion concentration ranging from 2.0 and 30.0 μM.

Driven by the situation that few fluorescent probes for Mg^{2+} were capable of applying in both animal cells and plant tissues, Zhou *et al.* developed **SBL-3**.[76] **SBL-3** shows high selectivity and sensitivity for the main group Mg^{2+} through fluorescence "turn-on" response in ethanol solution with no interference from Ca^{2+} in particular. Detection limit of probe **SBL-3** is 1.47×10^{-6} M and the rapid response could reach about 15–20 s. What's more, probe **SBL-3** presents great photostability, low toxicity, and cellular permeability and can successfully sense and detect Mg^{2+} in HeLa cells. Furthermore, it is successfully applied as a Mg^{2+} developer in plant tissues, indicating that it not only can successfully track the transport of Mg^{2+} but also is able to make a corresponding fluorescence response to different Mg^{2+} concentrations.

SBL-4 is an aggregation-induced emission (AIE)-active fluorescence probe.[77] It can be used as a sensitive probe to detect Mg^{2+} ion in acetonitrile and the other common ions shown no noticeable interference. Particularly, upon complexation with Mg^{2+}, the colour of the **SBL-4** solution changes from colourless to yellow under hand-held ultraviolet lamp, which can be observed by naked-eye. However, the biological application of probe **SBL-4** is limited by its inferior characteristics.

Interestingly, **SBL-5**, as described by Liu and colleagues, exhibits a solvent-dependent "turn-on" fluorescence recognition for Mg^{2+} anchored in combination of C=N isomerization as well as inhibition of ESIPT (the probable binding mode and action between **SBL-5** and Mg^{2+} are showed in Fig. 8).[78] The unique property of **SBL-5** is that it shows turn-on fluorescence response for Mg^{2+} only in alcohol solvent with sensitivity and negligible fluorescent response in other nonpolar or polar solvents. Upon binding with Mg^{2+}, a 148-fold fluorescence enhancement was observed at 458 nm when 20 μM Mg^{2+} was added, along with the colour changing from colourless to blue. However, due to these photophysical changes only happen in alcohol solvent, which is not close to the physiological environment, thus the probe might not be applied in colormetric and ratiometirc sensing of Mg^{2+} in living cells.

SBL-6, which was reported by Zhang*et al.* in 2017, is a novel "off–on" fluorescent probe based on 1, 8-naphthalimide derivative for the detection of Mg^{2+} in ethanol solution. The *o*-hydroxyl Schiff base, a very important unit in the structure of **SBL-6**, which not only plays the role of connecting 1,8-naphthalimide chromophore and 2-hydrazinylbenzo[D] thiazole group, but also acts as recognizer to realize "off–on" fluorescence recognition.[79] (The structure and proposed sensing process of **SBL-6** are showed in Fig. 8). Its complexation towards Mg^{2+} is a 1 : 2 binding mode in ethanol. **SBL-6** displays responses to Mg^{2+} with a fluorescence enhancement at 523 nm, accompanying with a distinct fluorescence change from nearly colorless to bright yellow-green. In addition, biological application experiments revealed that the probe is nearly non-toxic and the fluorescence scanning microscopic experiments demonstrated that the probe can be qualified for monitoring at the intracellular Mg^{2+} level successfully.

Recently, Li *et al.* designed, synthesized and evaluated **SBL-7** as a novel Mg^{2+} "turn on" fluorescent probe, which connected fluorescein-derived Schiff-base ligand to a chromone moiety.[80] **SBL-7** binds Mg^{2+} with good selectivity and exhibits excellent sensitivity towards Mg^{2+} over other important metal ions investigated. Upon binding with Mg^{2+}, the fluorescence emission intensity at 504 nm increases by about 50-fold. The remarkable enhancement in fluorescence emission is due to the fact that the ring opening process of the fluorescein fluorophore in **SBL-7** upon complexation with Mg^{2+}. **SBL-7** responses to Mg^{2+} within 3 min, and can be utilized to sense and monitor Mg^{2+} for real-time detection.

SBL-8 serves as a dual analyte probe and quantifies Mg^{2+} and Zn^{2+} ions, and that the binding constant of Mg^{2+} is lower.[81] It was designed and synthesized by Maity and his workmates using coumarin derivative 3-amino-7-(diethylamino)-2*H*-chromen-2-one as fluorophore and it was conjugated to 2,6-diformyl-4-methylphenol *via* a C=N bond as well. The proposed binding mode of **SBL-8** with Mg^{2+} and Zn^{2+} is based on C=N bond isomerisation mechanism and the binding sites maybe include the carbonyl oxygen of coumarin ring, imine nitrogen as well as phenolic oxygen (as shown in Fig. 8). However, owing to lack of selectivity towards Mg^{2+}, thus the application of **SBL-8** will be limited to some extent.

3.5 Miscellanea

As discussed in the preceding part of this review, four families of Mg^{2+}-responsive fluorescent probes have been reported and put into biological applications, *i.e.* the receptor groups based upon an APTRA, a charged β-diketone, a crown ether structure and a Schiff base ligand. However, there are still other types of Mg^{2+}-responsive fluorescent probes, which do not belong to the above classification, have also been developed. There-in-after, we will give a brief introduction of these probes.

Open Access Article. Published on 03 April 2018. Downloaded on 1/9/2025 5:36:55 PM. This article is licensed under a Creative Commons Attribution-NonCommercial 3.0 Unported Licence.

Calixarenes are cyclic oligomeric host molecules formed through a condensation reaction between phenol and formaldehyde. They exist in different ring sizes, each bearing a hydrophobic interior, among which the four-monomer ring system calix[4]arene is the most studied one. The usage of calix[4]arenediamide derivative as a probe for the detection of Mg^{2+} ions was described by Song and colleagues.[82] The probe exhibits a large Mg^{2+}-induced red-shifted emission. The selective sensing of Mg^{2+} over other potentially interfering ions could be realised by analysing the ratio between fluorescence emission at 493 and 409 nm, and the value was significantly higher for Mg^{2+}. Such discriminating behaviour suggested that this molecule could be utilized in ratiometric sensing of magnesium in semi-aqueous environments.

Analogously, porphyrins and their derivatives, which contain both a fluorophore and a coordination platform, are promising candidates for the development of cation-responsive probes. These molecules have ideal properties such as a cell-penetrating far-red or near-infrared fluorescent emission, as well as large Stokes shifts which minimize the influence of the background fluorescence.[83] In accordance with these superior features, a porphyrin-related macrocycle probe for Mg^{2+} recognition was proposed by Ishida and co-workers,[84] which also shows fluorescence enhancement and bathochromic shift upon Mg^{2+} complexation, while displaying inappreciable interference from other physiologically relevant cations (Na^+, K^+, Ca^{2+}). Thus it is recommended as a cell-permeable fluorescent sensor for Mg^{2+} in semi-aqueous solution enabling ratiometric measurements.

To the best of our knowledge, almost all fluorescent probes devised for the detection of Mg^{2+} meet a common problem of nonnegligible interference from either alkali metal ions or transition-metal ions. Fortunately, the use of a single-molecular multi-analyte, namely, a single probe that allows the sensing of multiple analytes with different spectral responses is promising for overcoming the poor selectivity of probe for Mg^{2+}. Inspired by this idea and towards this objective, two novel fluorescent probes, **KCM-1** and **DFC-8-AQ** (see in Fig. 9), were successfully designed, synthesized and characterized. **KCM-1**, one of single-molecular multi-analyte fluorescent probe for the simultaneous sensing of both Ca^{2+} and Mg^{2+}, was developed by Koji Suzuki and co-workers.[85] The molecule of novel probe **KCM-1** includes a coumarin moiety as a stable fluorophore which can be excited with visible light, BAPTA (*O*,*O*′-bis(2-aminophenyl)ethyleneglycol-*N*,*N*,*N*′,*N*′-tetraacetic acid) as the Ca^{2+}-selective binding site and a charged β-diketone as the Mg^{2+}-selective binding site. Consequently, fluorescence emission of **KCM-1** shows a spectral hypochromatic shift in the presence of Ca^{2+} and a bathochromic shift upon complexation to Mg^{2+}. Furthermore, Ca^{2+} and Mg^{2+} concentrations can be measured by a calibration performed on data acquired by a combination of three different excitation/emission wavelengths. However, the binding characteristics of **KCM-1** are quite disillusionary, as K_d values for Ca^{2+} and Mg^{2+} are reported to be 14 μM and 26 mM, respectively, which are obviously too high to effectively measure common intracellular concentrations of these ions. Nevertheless, **KCM-1** has been applied to detect distinct Ca^{2+} and Mg^{2+} transients upon mitochondrial depolarisation.

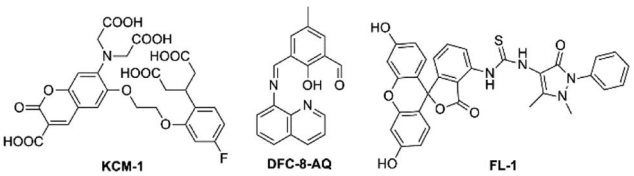

Fig. 9 Chemical structures of other types of Mg^{2+} probes.

The second probe in Fig. 9, **DFC-8-AQ** possesses a diformyl-*p*-cresol (DFC)-8-aminoquinoline moiety as the chromophore,[86] with the Schiff base linked to the benzene ring and the quinoline ring coupled with the phenolic and aldehyde groups to constitute the receptor moiety of the probe, which is very close to the charged β-diketone binding site. **DFC-8-AQ** displays colorimetric and fluorogenic properties upon selective and sensitive binding towards Mg^{2+} and Zn^{2+}. **DFC-8-AQ** turns on fluorescent enhancement as high as 40 folds and 53 folds upon binding of Mg^{2+} and Zn^{2+}, respectively. Additionally, this probe could be selective towards Mg^{2+} over Zn^{2+} in presence of the specific cell-permeable heavy metal chelator TPEN (*N*,*N*,*N*′,*N*′-tetrakis(2-pyridylmethyl)ethylenediamine), under both intra- and extracellular conditions. Furthermore the dissociation constant of the Mg^{2+}-(**DFC-8-AQ**) complex (K_d = 6.60 μM) is far lower than a large proportion of reported Mg^{2+} probes which fall in the mM range. However, despite the encouraging results, the project hasn't been pursued further yet.

A controlled supramolecular approach using allosteric effect in combination with conformation restriction in a fluorescein-based ring-off/open system was less investigated in the field of fluorescent probes. Yu *et al.* adopted this strategy to design and synthesize a novel fluorescent and colorimetric probe **FL-1** for Mg^{2+} or Ca^{2+} over other competing ions.[87] **FL-1** displays turn on fluorescent and colour changes upon addition of Mg^{2+} and Ca^{2+}. Through the experiments of fluorescence emission, UV-visible titrations and ^{1}H-NMR titrations revealed that the cation-driven can construct conformation of **FL-1**. And that Mg^{2+} and Ca^{2+} could be selectively sense by the allosteric effect. Even though this strategy is novel-innovative, one of its fatal drawbacks is that it cannot exclude the interference from Ca^{2+}.

4. Conclusions and outlook

In the present review, we attempt to cover the advances in fluorescent probes for detection of Mg^{2+} in past several decades, with the goal of providing some valuable clues to find the safe exit of such a colorful maze and direct future developments. Firstly, we placed emphasis on the discussion of general design principles of fluorescent probes for ion detection, which would contribute to the understanding of the operational mechanisms of fluorescent probes for both the users and the inventors. Simultaneously, we classified numerous fluorescent probes for sensing Mg^{2+} based on the structure of their recognition units. The appropriate combination of the ion acceptor unit and the fluorophore reporter unit can offer a potent tool for the visualisation of Mg^{2+} *in vitro* and *in vivo* to clarificate the roles of Mg^{2+} in living organisms. Since the pioneering work of

 This journal is © The Royal Society of Chemistry 2018

Open Access Article. Published on 03 April 2018. Downloaded on 1/9/2025 5:36:55 PM.
This article is licensed under a Creative Commons Attribution-NonCommercial 3.0 Unported Licence.

fluorescent probes for sensing intracellular Ca^{2+}, a multitude of fluorescent probes for the detection of Mg^{2+} have sprung up that operate according to various mechanisms and are constructed based on different chromophores in conjunction with multifarious selective-Mg^{2+} acceptors. Despite the rapid progress of Mg^{2+}-selective fluorescent probes, a diverse array of problems and challenges are shrouded in this research field at present. The current major knotty problems and challenges include:

4.1 Concerning the acceptor

A large proportion of Mg^{2+} probes suffer from the lack of selectivity over Ca^{2+} or other metal ions and the K_d value is relatively high. In addition, Mg^{2+} fluorescent probes which involve AM (acetoxymethyl) esters also have multiple problems, including compartmentalisation within intracellular organelles, incomplete hydrolysis resulting in the formation of fluorescent ion-insensitive species as well as leakage from cytosol to extracellular medium. Therefore, active search and creative development of acceptors with extraordinary affinity for Mg^{2+} without interference from competitive ions is in urgent demand. Meanwhile, further improvement of the acceptors would also contribute to their utility in cells.

4.2 In terms of the fluorophore

There is no doubt that the sensitivity and signal-to-noise ratio of a probe mainly depend on the brightness and stability of the probe's fluorophore(s) as well as the features of the instrumentation. In general, an ideal fluorophore should meet certain requirements, such as, (a) absorption and emission wavelengths in the visible region, or more preferably in near-infrared or infrared range; (b) good photo-stability and very low light scattering; (c) low or no toxicity to living cells; (d) excellent equilibrium between water soluble and fat-soluble property; (e) easy ways to produce and modify probes without high costs. However, the vast majority of fluorophores in Mg^{2+} fluorescent probes don't possess most of these elements, which drastically reduces the potential biological applications. Therefore, it is of highly priority to develop brighter fluorophores with better photo-physical nature.

4.3 Designing ratiometric probes or functional probes based on multi-sensing mechanisms

It is well-known that ratiometric fluorescent recognition prevails over conventional monitoring at a single wavelength since the method is free from the errors related to receptor concentration, photobleaching and environmental effects. Although it is an important step forward to develop control probes, ratiometric probes act as their own internal controls to correct potential dye-dependent localization and sample thickness effects. Such probes are allowed to evaluate the concentrations more quantitatively for Mg^{2+} buffered in the cell. The FRET probe for the detection of Mg^{2+} is currently blank, which is likely to be a future direction for effort. Besides, the combination of multi-responding mechanisms to construct functional probes will possibly be an ideal choice, too. Looking forward, it is obvious that the performance of probes designed by simultaneous multi-sensing mechanisms to elucidate interactions between Mg^{2+} pools and the living systems would be an attractive target in future.

4.4 Continued innovations in analytical methods and imaging techniques

Generally speaking, the possibility to monitor Mg^{2+} in a living organism would contribute significantly to magnesium research. Accordingly, the ultimate challenge is not only to design advanced probes, but also to develop satisfactory tools for *in vivo* investigations. Besides, an additional Frontier is to enlarge the toolkit for imaging Mg^{2+} in living organisms, this would undoubtedly enhance our comprehension of Mg^{2+} homeostasis at the organismal level. In the last decade, multitudes of different imaging techniques and analytical methods have been employed, ranging from wide-field fluorescence microscopy to confocal microscopy, from single photon fluorescence microscopy to two-photon fluorescence microscopy, and so on. It hopes that the spur that has inspired imaging techniques will also be passed on to the realm of magnesium research.

To sum up, we do believe that with on-limits attitude and extensive collaboration of researchers in chemistry, physics, medicine and biology, the design and synthesis of novel probes as well as the development of advanced imaging techniques and instrumentation will facilitate our understanding of the comprehensive role of Mg^{2+} in living cells.

Conflicts of interest

There are no conflicts to declare.

Acknowledgements

We are grateful for the financial supports from National Natural Science Foundation of China (81741134, 81671756, 81572946 and 81770739), Key Research Project of Science and Technology Foundation of Hunan Province (2017SK2090) and Fund of Changsha Science and Technology (kq1701018).

Notes and references

1 H. Rubin, *BioEssays*, 2005, **27**, 311–320.
2 A. M. Alexandra, *Sci. Signaling*, 2016, **9**, ec269.
3 M. H. Pontes, J. Yeom and E. A. Groisman, *Mol. Cell*, 2016, **64**, 480–492.
4 B. O'Rourke, P. H. Backx and E. Marban, *Science*, 1992, **257**, 245–248.
5 A. Romani, *Arch. Biochem. Biophys.*, 2007, **458**, 90–102.
6 F. I. Wolf and A. Cittadini, *Mol. Aspects Med.*, 2003, **24**, 3–9.
7 W. Jahnen-Dechent and M. Ketteler, *Clin. Kidney J.*, 2012, **5**, i3–i14.
8 J. F. Committee, *British National Formulary*, The Pharmaceutical Press, London, 2015, ISBN: 9780857111562, p. 463.
9 A. Walsh, *Spectrochim. Acta*, 1955, **7**, 108–117.

Open Access Article. Published on 03 April 2018. Downloaded on 1/9/2025 5:36:55 PM.
This article is licensed under a Creative Commons Attribution-NonCommercial 3.0 Unported Licence.

10 C. Feillet-Coudray, A. Trzeciakiewicz, C. Coudray, M. Rambeau, A. Chanson, Y. Rayssiguier, A. Opolski, F. I. Wolf and A. Mazur, *Eur. J. Nutr.*, 2006, **45**, 171–177.
11 H. R. Halvorson, A. M. Vande-Linde, J. A. Helpern and K. M. Welch, *NMR Biomed.*, 1992, **5**, 53–58.
12 S. Iotti and E. Malucelli, *Magnesium Res.*, 2008, **21**, 157–162.
13 H. Ishikawa, K. Suzuki, M. Nakanishi and A. Inokai, *Bioimaging for Molecular Dynamics and Cellular Functions*, Kyoritsushuppan Co., Ltd., Tokyo, 1998.
14 J. A. Thomas, *Chem. Soc. Rev.*, 2015, **44**, 4494–4500.
15 S. Lee, K. K. Yuen, K. A. Jolliffe and J. Yoon, *Chem. Soc. Rev.*, 2015, **44**, 1749–1762.
16 G. G. Guilbault, *Practical Fluorescence*, 2nd edn, Marcel Dekker Inc, New York, 1990, ISBN 0824783506.
17 A. P. de Silva, H. Q. Gunaratne, T. Gunnlaugsson, A. J. Huxley, C. P. McCoy, J. T. Rademacher and T. E. Rice, *Chem. Rev.*, 1997, **97**, 1515–1566.
18 N. Boens, V. Leen and W. Dehaen, *Chem. Soc. Rev.*, 2012, **41**, 1130–1172.
19 B. Valeur and I. Leray, *Coord. Chem. Rev.*, 2000, **205**, 3–40.
20 Z. R. Grabowski and J. Dobkowski, *Pure Appl. Chem.*, 1983, **55**, 245–252.
21 Y. M. Yang, Q. Zhao, W. Feng and F. Y. Li, *Chem. Rev.*, 2013, **113**, 192–270.
22 J. S. Kim and D. T. Quang, *Chem. Rev.*, 2007, **107**, 3780–3799.
23 J. Fan, M. Hu, P. Zhan and X. Peng, *Chem. Soc. Rev.*, 2013, **42**, 29–43.
24 Y. Feng, J. Cheng, L. Zhou, X. Zhou and H. Xiang, *Analyst*, 2012, **137**, 4885–4901.
25 A. Coskun and E. U. Akkaya, *J. Am. Chem. Soc.*, 2006, **128**, 14474–14475.
26 Y. Kurishita, T. Kohira, A. Ojida and I. Hamachi, *J. Am. Chem. Soc.*, 2010, **132**, 13290–13299.
27 R. Y. Tsien, *Biochemistry*, 1980, **19**, 2396–2404.
28 G. Grynkiewicz, M. Poenie and R. Y. Tsien, *J. Biol. Chem.*, 1985, **260**, 3440–3450.
29 L. A. Levy, E. Murphy, B. Raju and R. E. London, *Biochemistry*, 1988, **27**, 4041–4048.
30 B. Raju, E. Murphy, L. A. Levy, R. D. Hall and R. E. London, *Am. J. Physiol.*, 1989, **256**, C540–C548.
31 R. E. London, *Annu. Rev. Physiol.*, 1991, **53**, 241–258.
32 E. Murphy, C. C. Freudenrich, L. A. Levy, R. E. London and M. Lieberman, *Proc. Natl. Acad. Sci. U. S. A.*, 1989, **86**, 2981–2984.
33 R. M. Touyz and E. L. Schiffrin, *J. Biol. Chem.*, 1996, **271**, 24353–24358.
34 M. Tashiro, H. Inoue and M. Konishi, *Biophys. J.*, 2014, **107**, 2049–2058.
35 E. Gouadon, F. Lecerf and M. German-Fattal, *J. Pharm. Pharm. Sci.*, 2012, **15**, 389–398.
36 L. Csernoch, J. C. Bernengo, P. Szentesi and V. Jacquemond, *Biophys. J.*, 1998, **75**, 957–967.
37 C. Cheng and I. J., *Neurosciences*, 2000, **95**, 973–979.
38 L. S. Meena, S. R. Dhakate and P. D. Sahare, *Biotechnol. Appl. Biochem.*, 2012, **59**, 429–436.
39 Y. C. Lin, C. P. Broedersz, A. C. Rowat, T. Wedig, H. Herrmann, F. C. MacKintosh and D. A. Weitz, *J. Mol. Biol.*, 2010, **399**, 637–644.
40 M. Zhao, S. Hollingworth and S. M. Baylor, *Biophys. J.*, 1996, **70**, 896–916.
41 A. V. Shmigol, D. A. Eisner and B. Wray, *J. Physiol.*, 2001, **531**, 707–713.
42 Y. Sako, A. Sekihata, Y. Yanagisawa, M. Yamamoto, Y. Shimada, K. Ozaki and A. Kusumi, *J. Microsc.*, 1997, **185**, 9–20.
43 G. Q. Sun and R. J. A. Budde, *Biochemistry*, 1997, **36**, 2139–2146.
44 G. R. Budinger, J. Duranteau, N. S. Chandel and P. T. Schumacker, *J. Biol. Chem.*, 1998, **273**, 3320–3326.
45 T. W. Hurley, M. P. Ryan and R. W. Brinck, *Am. J. Physiol.*, 1992, **263**, C300–C307.
46 X. H. Dong, J. H. Han, C. H. Heo, H. M. Kim, Z. H. Liu and B. R. Cho, *Anal. Chem.*, 2012, **84**, 8110–8113.
47 H. J. Kim, J. H. Han, M. K. Kim, C. S. Lim, H. M. Kim and B. R. Cho, *Angew. Chem., Int. Ed.*, 2010, **49**, 6786–6789.
48 H. M. Kim, C. Jung, B. R. Kim, S. Y. Jung, J. H. Hong, Y. G. Ko, K. J. Lee and B. R. Cho, *Angew. Chem., Int. Ed.*, 2007, **46**, 3460–3463.
49 M. S. Afzal, J. P. Pitteloud and D. Buccella, *Chem. Commun.*, 2014, **50**, 11358–11361.
50 J. J. Gruskos, G. Q. Zhang and D. Buccella, *J. Am. Chem. Soc.*, 2016, **138**, 14639–14649.
51 Y. Suzuki, H. Komatsu, T. Ikeda, N. Saito, S. Araki, D. Citterio, H. Hisamoto, Y. Kitamura, T. Kubota, J. Nakagawa, K. Oka and K. Suzuki, *Anal. Chem.*, 2002, **74**, 1423–1428.
52 E. J. Park, M. Brasuel, A. P. Martin and R. Kopelman, *Anal. Chem.*, 2003, **75**, 3784–3791.
53 A. Minta, J. P. Kao and R. Y. Tsien, *J. Biol. Chem.*, 1989, **264**, 8171–8178.
54 T. Shoda, K. Kikuchi, H. Kojima, Y. Urano, H. Komatsu, K. Suzuki and T. Nagano, *Analyst*, 2003, **128**, 719–723.
55 H. Komatsu, N. Iwasawa, D. Citterio, Y. Suzuki, T. Kubota, K. Tokuno, Y. Kitamura, K. Oka and K. Suzuki, *J. Am. Chem. Soc.*, 2004, **126**, 16353–16360.
56 Y. Shindo, T. Fujii, H. Komatsu, D. Citterio, K. Hotta, K. Suzuki and K. Oka, *PLoS One*, 2011, **6**, e23684.
57 T. Kubota, Y. Shindo, K. Tokuno, H. Komatsu, H. Ogawa, S. Kudo, Y. Kitamura, K. Suzuki and K. Oka, *Biochim. Biophys. Acta*, 2005, **1744**, 19–28.
58 T. Fujii, Y. Shindo, K. Hotta, D. Citterio, S. Nishiyama, K. Suzuki and K. Oka, *J. Am. Chem. Soc.*, 2014, **136**, 2374–2381.
59 H. M. Kim, P. R. Yang, M. S. Seo, J. S. Yi, J. H. Hong, S. J. Jeon, Y. G. Ko, K. J. Lee and B. R. Cho, *J. Org. Chem.*, 2007, **72**, 2088–2096.
60 V. K. Gupta, N. Mergu, L. K. Kumawat and A. K. Singh, *Sens. Actuators, B*, 2015, **207**, 216–223.
61 H. Hama, T. Morozumi and H. Nakamur, *Tetrahedron Lett.*, 2007, **48**, 1859–1861.
62 K. Soroka, R. S. Vithanage, D. A. Phillips, B. Walker and P. K. Dasgupta, *Anal. Chem.*, 1987, **59**, 629–636.

 This journal is © The Royal Society of Chemistry 2018

Open Access Article. Published on 03 April 2018. Downloaded on 1/9/2025 5:36:55 PM.
This article is licensed under a Creative Commons Attribution-NonCommercial 3.0 Unported Licence.

63 I. Devol and E. J. Bardez, *J. Colloid Interface Sci.*, 1998, **200**, 241–248.
64 L. Prodi, M. Montalti, J. S. Bradshaw, R. M. Izatt and P. B. Savage, *J. Inclusion Phenom. Macrocyclic Chem.*, 2001, **41**, 123–127.
65 L. Prodi, F. Bolletta, M. Montalti, N. Zaccheroni, P. B. Savage, J. S. Bradshaw and R. M. Izatt, *Tetrahedron Lett.*, 1998, **39**, 5451–5454.
66 G. Farruggia, S. Iotti, L. Prodi, M. Montalti, N. Zaccheroni, P. B. Savage, V. Trapani, P. Sale and F. I. Wolf, *J. Am. Chem. Soc.*, 2006, **128**, 344–350.
67 G. Farruggia, S. Iotti, L. Prodi, N. Zaccheroni, M. Montalti, P. B. Savage, G. Andreani, V. Trapani and F. I. Wolf, *J. Fluoresc.*, 2009, **19**, 11–19.
68 C. Marraccini, G. Farruggia, M. Lombardo, L. Prodi, M. Sgarzi, V. Trapani, C. Trombini, F. I. Wolf, N. Zaccheroni and S. Iotti, *Chem. Sci.*, 2012, **3**, 727–734.
69 A. Sargenti, G. Farruggia, N. Zaccheroni, C. Marraccini, M. Sgarzi, C. Cappadone, E. Malucelli, A. Procopio, L. Prodi, M. Lombardo and S. Iotti, *Nat. Protoc.*, 2017, **12**, 461–471.
70 A. Casnati, F. Sansone, A. Sartori, L. Prodi, M. Montalti, N. Zaccheroni, F. Ugozzoli and R. Ungaro, *Eur. J. Org. Chem.*, 2003, **2003**, 1475–1485.
71 O. Seneque and J. M. Latour, *J. Am. Chem. Soc.*, 2010, **132**, 17760–17774.
72 L. Lvova, C. G. Gonçalves, L. Prodi, M. Sgarzi, N. Zaccheroni, M. Lombardo, A. Legin, C. D. Natale and R. Paolesse, *Anal. Chim. Acta*, 2017, **988**, 96–103.
73 R. Hernández-Molina and A. Mederos, in *Comprehensive Coordination Chemistry II*, 2004, vol. 1, pp. 411–446, ISBN: 978-0-08-043748-4.
74 D. Ray and P. K. Bharadwaj, *Inorg. Chem.*, 2008, **47**, 2252–2254.
75 N. Singh, N. Kaur, R. C. Mulrooney and J. F. Callan, *Tetrahedron Lett.*, 2008, **49**, 6690–6692.
76 T. T. Yu, P. Sun, Y. J. Hu, Y. G. Ji, H. P. Zhou, B. W. Zhang, Y. P. Tian and J. Y. Wu, *Biosens. Bioelectron.*, 2016, **86**, 677–682.
77 Y. J. Bian, L. Q. Wang, F. X. Cao and L. J. Tang, *J. Fluoresc.*, 2016, **26**, 53–57.
78 Z. D. Liu, H. J. Xu, S. S. Chen, L. Q. Sheng, H. Zhang, F. Y. Hao, P. F. Su and W. L. Wang, *Spectrochim. Acta, Part A*, 2015, **149**, 83–89.
79 H. F. Zhang, C. X. Yin, T. Liu, J. B. Chao, Y. B. Zhang and F. J. Huo, *Dyes Pigm.*, 2017, **146**, 344–351.
80 C. R. Li, S. L. Li, G. Q. Wang and Z. Y. Yang, *J. Photochem. Photobiol. A: Chem.*, 2018, **356**, 700–707.
81 S. B. Maity and P. K. Bharadwaj, *J. Lumin.*, 2014, **155**, 21–26.
82 K. C. Song, M. G. Choi, D. H. Ryu, K. N. Kim and S. K. Chang, *Tetrahedron Lett.*, 2007, **48**, 5397–5400.
83 K. M. Kadish, K. M. Smith and R. Guilard, Applications of Phthalocyanines, *The Porphyrin Handbook*, Academic Press, New York, 1st edn, 2003.
84 M. Ishida, Y. Naruta and F. Tani, *Angew. Chem., Int. Ed.*, 2010, **49**, 91–94.
85 H. Komatsu, T. Miki, D. Citterio, T. Kubota, Y. Shindo, Y. Kitamura, K. Oka and K. Suzuki, *J. Am. Chem. Soc.*, 2005, **127**, 10798–10799.
86 R. Alam, T. Mistri, A. Katarkar, K. Chaudhuri, S. K. Mandal, A. R. Khuda-Bukhsh, K. K. Das and M. Ali, *Analyst*, 2014, **139**, 4022–4030.
87 X. D. Y., P. Zhang, Q. R. Liu, Y. J. Li, X. L. Zhen, Y. M. Zhang and Z. C. Ma, *Mater. Sci. Eng., C*, 2014, **39**, 73–77.